Supplemental Material to "Universal relations between thermoelectrics and noise in mesoscopic transport across a tunnel junction"

Andrei I. Pavlov[1, *] and Mikhail N. Kiselev[2]

[1] *IQMT, Karlsruhe Institute of Technology, 76131 Karlsruhe, Germany*
[2] *The Abdus Salam International Centre for Theoretical Physics, Strada Costiera 11, I-34151 Trieste, Italy*

I. CONNECTION BETWEEN CONSIDERED MODEL AND REALISTIC EXPERIMENTAL SETUPS

In the section, we provide a detailed explanation of the connection between our considered model and realistic experimental setups.
As an experimental setup for our theoretical analysis, we assume a well-established method of scanning tunnel microscope (STM) probe of the system where the probe's temperature can be different from the temperature of the reference system. The Johnson-Nyquist noise, shot noise, delta-T noise can be reliably measured through a tunnel junction, e. g., [1–3], including the STM break junction [4] (this work also discusses applications of this experimental technique for local measurements of shot noise in non-Fermi liquids).
We consider a lead of normal metal (Fermi liquid) serving as a probe, while the reference system (which is probed by the "tip" of the STM) is arbitrary (not necessarily a Fermi liquid). The important assumption is that the temperature and voltage drop occur across the tunnel junction. We are dealing with a weak out-of-equilibrium conditions (zero bias). Corresponding currents (charge and heat) are also vanishing. The metallic (macroscopic) lead is characterized by its chemical potential and temperature. This setup is illustrated in Fig. S1. The probed system may have some nontrivial internal structure, however, the tunnel junction transmission coefficient is determined solely by the local density of states at the tunnel junction.

A paradigmatic example of such a system is a charge Kondo circuit [5–9]. In this mesoscopic device, a central island (a metallic quantum dot) is connected to one or several quantum point contacts (QPCs). This island exhibits a weak charge quantization operating in a mesoscopic Coulomb blockade regime. The charge quantization allows to fine tune the nano-device (by means of gate voltages applied to the QPCs) to a charge degeneracy point where the charge Kondo effect emerges. Pronounce fingerprints of the non-Fermi liquid behavior associated with multi-channel charge Kondo effect within the central island have been demonstrated experimentally [10, 11]. The design of these experiments assumes that the voltage probe is taken far away from the QPC where the system already transitioned

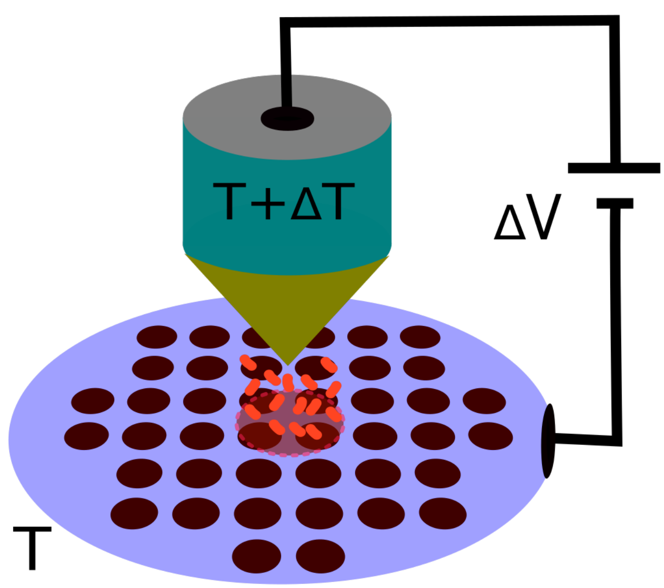

FIG. S1. Considered setup: A system with some inner structure (light blue with dark dots) at temperature T is coupled through a tunnel junction (red) to a metallic lead (teal and olive) at temperature $T + \Delta T$ serving as a probe. Additionally, there is a voltage bias ΔV induced between the system and the probe. The current and noise observables are governed by the local density of states in the probed system (red circle).

(through a crossover) to the Fermi liquid metallic regime, and the distribution function of the electrons is given by the Fermi distribution function. At the distances much larger than the size of the QD-QPC area, the temperature and chemical potential can be attributed to corresponding Fermi system, so the quantum dot in such a device has well-defined temperature and chemical potential. An STM probe can be applied to the central island of this mesoscopic device (or one of the QPCs in this setup can be pinched to make a tunnel junction, probing a QD connected to a single QPC, along the original proposals for the charge Kondo circuit [5–9]). The effects of the strong electron-electron correlations and resonance scattering occurring at the QD-QPC strongly renormalize the transmission coefficient across the tunnel junction, and as a result affect the quantum transport (namely, charge and heat currents and voltage and temperature driven charge, heat and mixed noises) through the junction.

Recent STM experimental probes of the fractional quantum Hall states [12, 13] are another example of the non-Fermi liquid investigation in the considered STM setup. Despite a complex structure of the investigated system, only the integrated density of states under the STM tip contributes to the measurements.

The considered STM setup is also essential for observations of the transport signatures of the Sachdev-Ye-Kitaev (SYK) model in a proposed experimental realizations of this model in a disordered graphene flake [14].

II. RESONANT LEVEL MODEL

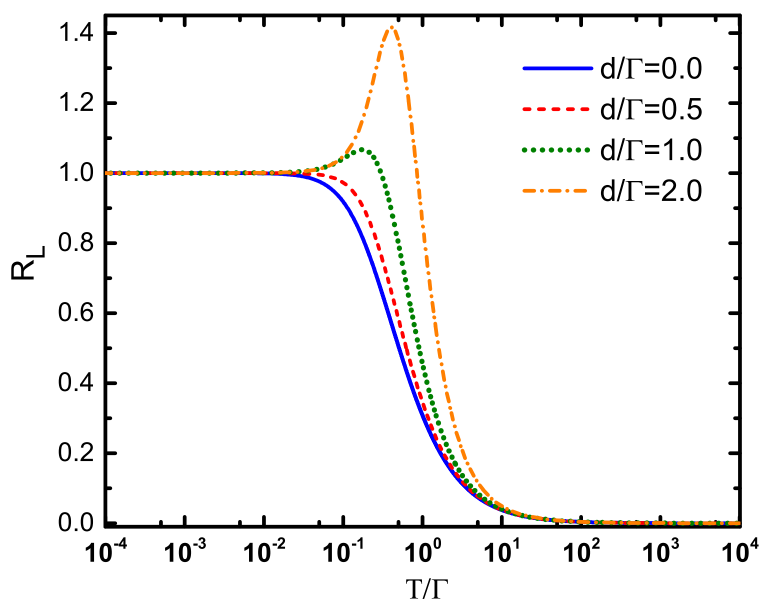

FIG. S2. Lorenz ratio R_L of the resonant impurity model as function of temperature for various spectral asymmetries. Solid blue line: $d/\Gamma = 0$; dashed red line: $d/\Gamma = 0.5$, dotted green line: $d/\Gamma = 1$; dot-dashed orange line: $d/\Gamma = 2$.

In this section, we provide analytical analysis of the transport coefficients for the resonant level model. The transmission coefficient of the resonant level model reads [15]

$$T(\varepsilon) \sim \frac{\Gamma^2}{\Gamma^2 + (\varepsilon - d)^2}, \tag{S1}$$

Γ is the width of the resonant level, d is the energy shift inducing the spectral asymmetry. Using Eq. (4) of the main text, we can calculate the transport coefficients. The advantage of this integrable model is that it allows for analytical calculations in all regimes. By introducing $x = \Gamma/T$, $\tilde{d} = d/T$ we have

$$\mathcal{L}_0 = \frac{1}{4}\int dz \frac{x^2}{x^2 + (z - \tilde{d})^2} \frac{1}{\cosh^2(\frac{z}{2})} = \frac{\Gamma}{4\pi T}\left[\psi^{(1)}\left(\frac{1}{2} + \frac{\Gamma + id}{2\pi T}\right) + \psi^{(1)}\left(\frac{1}{2} + \frac{\Gamma - id}{2\pi T}\right)\right], \tag{S2}$$

where $\psi^{(1)}(y) = \sum_{n=0}^{\infty} \frac{1}{(n+y)^2}$ is the trigamma function. The detailed analytical evaluation of integrals of such structure can be found in [16, 17].

$$\mathcal{L}_2 = \frac{T^2}{4}\int dz \frac{x^2}{x^2+(z-\tilde{d})^2}\frac{z^2}{\cosh^2(\frac{z}{2})} = \frac{T^2x^2}{4}\int dz\left(1-\frac{x^2+\tilde{d}^2-2z\tilde{d}}{x^2+(z-\tilde{d})^2}\right)\frac{1}{\cosh^2(\frac{z}{2})} = \Gamma^2 - \frac{\Gamma}{4\pi T}\left[(\Gamma+id)^2\psi^{(1)}\left(\frac{1}{2}+\frac{\Gamma+id}{2\pi T}\right)+(\Gamma-id)^2\psi^{(1)}\left(\frac{1}{2}+\frac{\Gamma-id}{2\pi T}\right)\right]. \tag{S3}$$

As is evident there, there are two regimes where the generalized WF law is obeyed. Namely, it is satisfied in the regime $T/\Gamma \ll 1$, with the Lorenz ratio reproducing the Fermi-liquid results $R_L = 1$ (in this regime, only $\varepsilon \ll \Gamma$ energies contribute to $\mathcal{L}_0$ and $\mathcal{L}_2$, so the transmission coefficient Eq. (S1) can by approximated by a constant, corresponding to the $\alpha = 1$ case of Eq. (10) in the main text). The generalized WF law is further obeyed in the high temperature limit $T/\Gamma \gg 1$ with the Lorenz ratio converging to $R_L = 0$. As expected, the generalized WL is violated at the intermediate temperature scales $T/\Gamma \sim 1$, where the integrals (S2), (S3) cannot be approximated as single-scale functions.

For completeness, let's write here the exact expression for the $\mathcal{L}_1$ integral,

$$\mathcal{L}_1 = \frac{T}{4}\int dz \frac{x^2}{x^2+(z-\tilde{d})^2}\frac{z}{\cosh^2\left(\frac{z}{2}\right)} = \frac{\Gamma}{4\pi T}\left[(d-i\Gamma)\psi^{(1)}\left(\frac{1}{2}+\frac{\Gamma+id}{2\pi T}\right)+(d+i\Gamma)\psi^{(1)}\left(\frac{1}{2}+\frac{\Gamma-id}{2\pi T}\right)\right]. \tag{S4}$$

With this, one can explicitly calculate the experimentally motivated WF-law ratio $\kappa/(TG)$ (the WF law measured at the zero electric current condition). It has exactly the same validity range and high-T, low-T Lorenz ratio values as $G_H/(TG)$ plotted in Fig. S2, with only differences appearing in the non-universal regime $T \sim \Gamma$, where the generalized WF law is violated.

III. COMPETITION BETWEEN DIFFERENT ENERGY SCALES

While the transmission coefficient scaling $\mathcal{T}\left(\frac{1}{2T}+it\right) \sim \frac{1}{\cosh^{\alpha}(\pi T t)}$ captures limiting cases of a wide variety of quantum impurity systems discussed in the main text, the presented theory can be employed to calculate the noise components in arbitrary cases. Here, we demonstrate how the cosh-scaling satisfies the limiting cases in the exact analysis of the two-channel charge Kondo system.

For the two-channel charge Kondo system (2CK), the transmission coefficient is known analytically [17–19]. The density of states of the 2CK dot can be decomposed to even and odd components, $\nu(\varepsilon) = \nu^e(\varepsilon) + \nu^o(\varepsilon)$, these components are explicitly given in [19]. Up to constant terms (that cancel out in the ratios of the noise integrals), these components are

$$\nu^e(\varepsilon) \sim \int dx \frac{\cosh\left(\frac{\varepsilon}{2T}\right)}{\cosh\frac{x}{2}}\frac{p}{x^2+p^2}\frac{x+\varepsilon/T}{\sinh\left(\frac{x+\varepsilon/T}{2}\right)}, \tag{S5}$$

$$\nu^o(\varepsilon) \sim \int dx \frac{\cosh\left(\frac{\varepsilon}{2T}\right)}{\cosh\frac{x}{2}}\frac{x}{x^2+p^2}\frac{x+\varepsilon/T}{\sinh\left(\frac{x+\varepsilon/T}{2}\right)}, \tag{S6}$$

where $p = \Gamma/T$, and Γ is the Kondo-resonance width. For $T \gg \Gamma$, the system is in the non-Fermi liquid regime (corresponding to $\alpha = 2$), while for $T \ll \Gamma$, the system exhibits the local Fermi-liquid behavior (the same as in the one-channel charge Kondo (1CK) $\alpha = 3$). At the intermediate energy scale $T \simeq \Gamma$, there is a crossover between the two phases which has non-universal behavior. We use Eqs. (S5) and (S6) to calculate the symmetric and antisymmetric coefficients through Eqs. (4), (5) of the main text, and plot the ratios between different integrals in Fig. S3. As expected, the WF law and all the universal noise relations are obeyed in two limiting cases, $T \gg \Gamma$ (2CK) and $T \ll \Gamma$ (1CK), where the transmission coefficient scaling becomes a single-parameter function. In Table S1, we provide the values of the corresponding ratios. For the symmetric coefficients, the agreement with the extended Lorenz numbers for symmetric coefficients from the main text is perfect. For the antisymmetric coefficients, there is a small discrepancy between these exact numerical results and the estimates given in the main text (0.826 vs 0.852 for 2CK, 0.760 vs 0.784 for 1CK) and Eq. (15) (1.485 vs 1.400 for 2CK, 1.715 vs 1.625 for 1CK). The reason for that is the approximation used for the odd component of the transmission coefficient (which has more complicated structure, in general, than the even component [20]). Nevertheless, this simple estimate provides us with the results

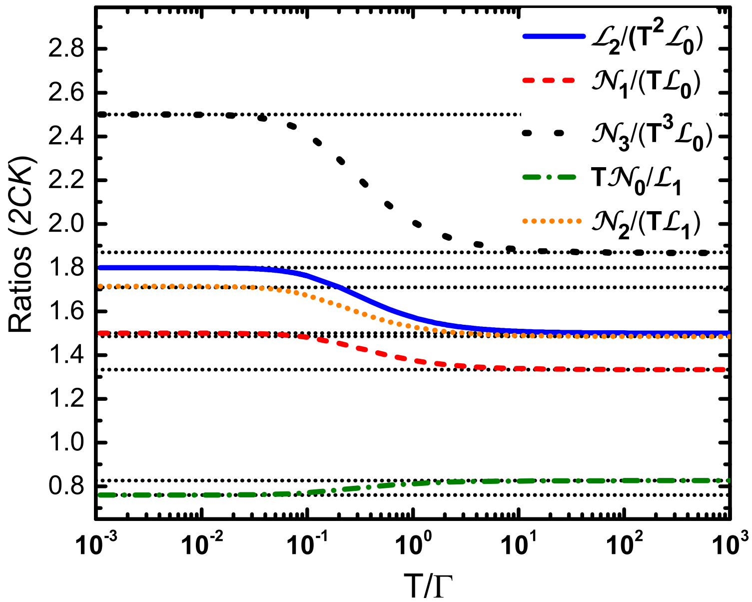

FIG. S3. Ratios between transport and noise integrals for a two-channel charge Kondo (2CK) system.

	$\frac{\mathcal{L}_2}{T^2\mathcal{L}_0}$	$\frac{\mathcal{N}_1}{T\mathcal{L}_0}$	$\frac{\mathcal{N}_3}{T^3\mathcal{L}_0}$	$\frac{T\mathcal{N}_0}{\mathcal{L}_1}$	$\frac{\mathcal{N}_2}{T\mathcal{L}_1}$
2CK ($\alpha = 2$)	$\frac{3}{2}$	$\frac{4}{3}$	$\frac{28}{15}$	0.826	1.485
1CK ($\alpha = 3$)	$\frac{9}{5}$	$\frac{3}{2}$	$\frac{5}{2}$	0.760	1.715

TABLE S1. Extended Lorenz ratios for the 2CK, 1CK systems.

within $\lesssim 5\%$ relative error for the numerical values between the universally related antisymmetric transport and noise integrals. At the intermediate energy scales, $T \simeq \Gamma$, the WF breaks, and all the noise relations break along with it too. This happens due to the energy scale Γ which violates the single-parametric scaling of the transmission coefficient as elaborated in the main text.
A similar analysis for the SYK dot is provided in [21]. The single-parametric scaling is broken in that case by the Coulomb blockade E_C, so the WF law and the noise relations break at $T \simeq E_C$, while they are obeyed in the $T \gg E_C$ and $T \ll E_C$ regimes, in accordance with our predictions.

IV. TWO-STAGE KONDO EFFECT

In this section, we demonstrate the Wiedemann-Franz (WF) law (and other universal ratios) for two different stages of the two-stage Kondo effect [22] recently observed experimentally [23], and the WF law violation on the intermediate scales in such a system. Generally, a two-level quantum dot may have the Coulomb interaction term U, so such a system needs to be treated numerically for obtaining quantitative results [24]. For the $U = 0$ case, however, the model is non-interacting and its transmission coefficient can be written exactly. In particular, let us consider two quantum dots coupled to metallic leads in a T-shaped configuration (the first dot is directly coupled to both leads, the second dot is coupled only to the first dot). The transmission coefficient for such a system at $U = 0$ for both dots reads [25]

$$\mathcal{T}(\varepsilon) = \frac{\Gamma^2}{\Gamma^2 + (\varepsilon - d - \frac{g^2}{\omega - a})^2}, \qquad \text{(S7)}$$

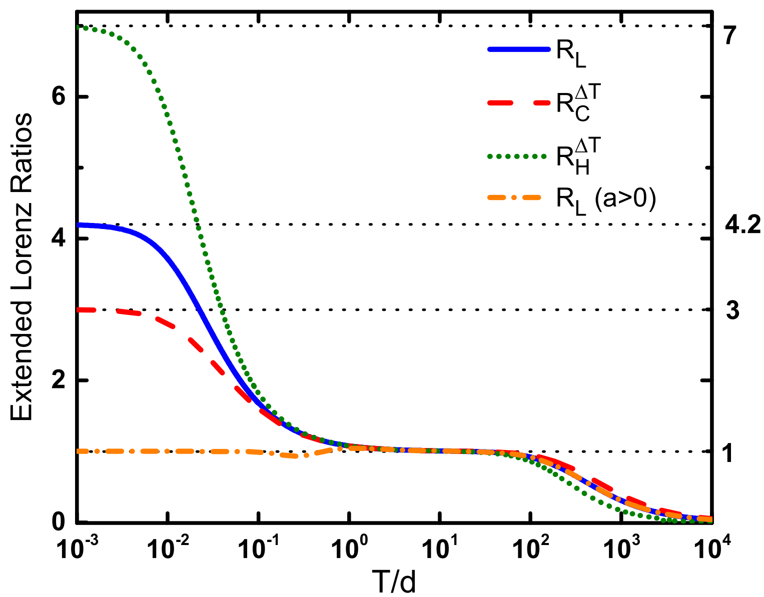

FIG. S4. Extended Lorenz ratios $R_L, R_C^{\Delta T}, R_H^{\Delta T}$ of the two-stage Kondo system as functions. Solid blue line: R_L; dashed red line: $R_C^{\Delta T}$; dotted green line: $R_H^{\Delta T}$. $\Gamma/d = 10^3$, $g/d = 10$, $a/d = 0$. Dot-dashed range line: the Lorenz ratio R_L for the same parameters except $a/d = 1$.

where Γ is hybridization of the first dot with the leads, d is the energy of the first dot, a is the energy of the second dot (not coupled to the leads directly), g is the hopping amplitude between the two dots. g and Γ are independent quantities that, in general, can have an arbitrary ratio. We assume $g \ll \Gamma$ for illustrative purposes.

The Kondo screening occurs in such a system in two stages. At the first stage, the spin of the first impurity (the one directly coupled to the leads) is screened, which happen at temperatures $g \ll T \ll \Gamma$. In this regime, the transmission coefficient (S7) can be effectively approximated as a constant. This immediately provides us with the Lorenz ratio of the Fermi liquid $R_L = 1$ (and the corresponding set of the extended Lorenz ratios). The second stage occurs at the low temperature regime $T \ll g$, where the second dot gets screened. In this regime, the transmission coefficient (S7) behaves as $\mathcal{T}(\varepsilon) \sim \varepsilon^2$ if $a = 0$ in Eq. (S7), or $\mathcal{T}(\varepsilon) \sim const$ if $a \neq 0$ (see also [26]). This effective transmission coefficient ensures that the transport integrals behave as single-scaling functions, so the generalized Wiedemann-Franz law is obeyed again. Due to the dip in the DoS in the $a = 0$ case, the Lorenz ratio gets boosted, as discussed in the main text. Namely, $R_L = \frac{21}{5}$ was found in [26]. Between these two universal regimes, the generalized WF law is violated, as expected from the fact that the transmission coefficient in this transitional regime depends on several energy parameters. In Fig. S4, we demonstrate the extended Lorenz ratios between the symmetric transport coefficients. At the first stage of the screening (which takes place at intermediate temperatures), they all saturate to the Fermi-liquid value ($R_L = R_C^{\Delta T} = R_H^{\Delta T} = 1$), while at the second stage they saturate to their specific values. In this regime, their limiting values are

$$R_L = \frac{3}{\pi^2} \frac{\int dz \frac{z^4}{\cosh\left(\frac{z}{2}\right)}}{\int dz \frac{z^2}{\cosh\left(\frac{z}{2}\right)}} = \frac{21}{5}, \tag{S8}$$

$$R_C^{\Delta T} = \frac{\int dz \frac{z^3 \tanh\left(\frac{z}{2}\right)}{\cosh\left(\frac{z}{2}\right)}}{\int dz \frac{z^2}{\cosh\left(\frac{z}{2}\right)}} = 3, \tag{S9}$$

$$R_C^{\Delta T} = \frac{1}{\pi^2} \frac{\int dz \frac{z^5 \tanh\left(\frac{z}{2}\right)}{\cosh\left(\frac{z}{2}\right)}}{\int dz \frac{z^2}{\cosh\left(\frac{z}{2}\right)}} = 7. \tag{S10}$$

As is evident from Fig. S4, the extended Lorenz ratios indeed converge to these values in the zero-temperature limit. For completeness, we provide here also the universal ratios between the antisymmetric transport coefficients using the exact expression Eq. (S7) (in the low-temparature limit, the leading contribution to the antisymmetric transmission coefficient at $a = 0$ is $\mathcal{T}^{odd}(\varepsilon) \sim \varepsilon^3$):

$$L_3 R_C^V = \frac{T\mathcal{N}_0}{\mathcal{L}_1} = \frac{15}{7\pi^2}, \tag{S11}$$

$$L_4 R_H^V = \frac{\mathcal{N}_2}{T\mathcal{L}_1} = 5. \tag{S12}$$

V. BEYOND LINEAR RESPONSE

Here we discuss how the universal relations between currents and noise can be extended beyond the linear response regime.
We denote the Fermi-Dirac distribution function of the system and the lead, correspondingly, as $n_S = f(\varepsilon)$ and $n_L = f(\varepsilon) + \Delta f(\varepsilon)$. The general expression for currents is

$$I_n = \int d\varepsilon (\varepsilon - V)^n \nu_S(\varepsilon)\nu_L \Delta f(\varepsilon), \tag{S13}$$

where $n = 0, 1$ for charge and heat current correspondingly. Using Eq. (2), and rewriting

$$n_L + n_S - 2n_L n_S = 2f(\varepsilon)\left[1 - f(\varepsilon)\right] + \Delta f(\varepsilon)\left[1 - 2f(\varepsilon)\right],$$

one gets the equilibrium noise (contribution from the first term) and the excess noise (the second term), which is

$$\Delta S_l = \int d\varepsilon (\varepsilon - V)^l \nu_S(\varepsilon)\nu_L \tanh\left(\frac{\varepsilon}{2T}\right)\Delta f(\varepsilon), \tag{S14}$$

$l = 0, 1, 2$ for the charge, mixed and heat noise, and we used $1 - 2f(\varepsilon) = \tanh\frac{\varepsilon}{2T}$, T is the temperature of the system.

Let us consider transport coefficients with respect to second derivatives. I. e., we analyze components of currents and noise in the second order of biases, $(\Delta V)^2, (\Delta T)^2, \Delta V \Delta T$ [27, 28]. For the currents, all the components can be expressed in the closed form through the linear response transport and noise coefficients:

$$\frac{\partial^2 I_c}{\partial V^2} = \frac{\mathcal{N}_0}{T}, \tag{S15}$$

$$\frac{\partial^2 I_c}{\partial V \partial(\Delta T)} = \frac{\mathcal{N}_1}{T^2} - \frac{\mathcal{L}_0}{T}, \tag{S16}$$

$$\frac{\partial^2 I_c}{\partial(\Delta T)^2} = \frac{\mathcal{N}_2}{T^3} - 2\frac{\mathcal{L}_1}{T^2}, \tag{S17}$$

$$\frac{\partial^2 I_h}{\partial V^2} = \frac{\mathcal{N}_1}{T} - 2\mathcal{L}_0, \tag{S18}$$

$$\frac{\partial^2 I_h}{\partial V \partial(\Delta T)} = \frac{\mathcal{N}_2}{T^2} - 2\frac{\mathcal{L}_1}{T}, \tag{S19}$$

$$\frac{\partial^2 I_h}{\partial(\Delta T)^2} = \frac{\mathcal{N}_3}{T^3} - \frac{\mathcal{L}_2}{T^2}. \tag{S20}$$

We can further write expressions for the second order noise derivatives. For that purpose, it's convenient to introduce a new type of noise integrals (second order noise integrals)

$$\mathcal{D}_n = \frac{1}{4T}\int d\varepsilon \mathcal{T}(\varepsilon)\frac{\varepsilon^n \tanh^2\left(\frac{\varepsilon}{2T}\right)}{\cosh^2\left(\frac{\varepsilon}{2T}\right)}, \quad n = 0, .., 4. \tag{S21}$$

Note that, akin to the transport integrals $\mathcal{L}_n$, even integrals $\mathcal{D}_n$ are symmetric with respect to the contributions from the $\mathcal{T}(\varepsilon)$, while odd integrals are antisymmetric (for the $\mathcal{N}_0$ integrals, the situation is the opposite).

$$\frac{\partial^2 S_c}{\partial V^2} = \frac{1}{T}\mathcal{D}_0, \tag{S22}$$

$$\frac{\partial^2 S_c}{\partial V \partial(\Delta T)} = \frac{1}{T^2}\mathcal{D}_1 - \frac{1}{T}\mathcal{N}_0, \tag{S23}$$

$$\frac{\partial^2 S_c}{\partial(\Delta T)^2} = \frac{1}{T^3}\mathcal{D}_2 - \frac{2}{T^2}\mathcal{N}_1, \tag{S24}$$

$$\frac{\partial^2 S_h}{\partial V^2} = \frac{1}{T}\mathcal{D}_2 - 4\mathcal{N}_1, \tag{S25}$$

$$\frac{\partial^2 S_h}{\partial V \partial(\Delta T)} = \frac{1}{T^2}\mathcal{D}_3 - \frac{3}{T}\mathcal{N}_2, \tag{S26}$$

$$\frac{\partial^2 S_h}{\partial(\Delta T)^2} = \frac{1}{T^3}\mathcal{D}_4 - \frac{2}{T^2}\mathcal{N}_3. \tag{S27}$$

Similar to the linear response regime, the mixed noise components do not bring us any new information about the system and can be fully expressed through components of charge and heat noise.

$$\frac{\partial^2 S_m}{\partial V^2} = \frac{1}{T}\mathcal{D}_1 - 2\mathcal{N}_0, \tag{S28}$$

$$\frac{\partial^2 S_m}{\partial V \partial(\Delta T)} = \frac{1}{T^2}\mathcal{D}_2 - \frac{2}{T}\mathcal{N}_1, \tag{S29}$$

$$\frac{\partial^2 S_m}{\partial(\Delta T)^2} = \frac{1}{T^3}\mathcal{D}_3 - \frac{2}{T^2}\mathcal{N}_2. \tag{S30}$$

From the expressions for non-linear current and noise components, one can construct multiple universal ratios and reciprocity relations which have the same applicability range as linear response results of the main text. For instance, one can consider the generalized Fano factor [27, 29], defined as the ratio between the corresponding components of the noise and currents with a subtraction of the linear response contributions. For the charge current noise due to voltage bias, we have

$$\delta F_c^{SN} = \left.\frac{\Delta S_c - \Delta S_c^{lin}}{I_c - I_c^{lin}}\right|_{\Delta T=0} = \frac{\mathcal{D}_0}{\mathcal{N}_0}, \tag{S31}$$

$$\delta F_c^{SN} F_c^{SN} = \frac{\mathcal{D}_0}{\mathcal{N}_0}\frac{\mathcal{N}_0}{\mathcal{L}_0} = \frac{\mathcal{D}_0}{\mathcal{L}_0}. \tag{S32}$$

Therefore, the product of the Fano factor and the generalized Fano factor becomes a universal constant. For instance, for the Fermi liquid ($\mathcal{T}(\varepsilon) = const$, or equivalently $\mathcal{T}\left(\frac{1}{2T} + it\right) \sim \cosh^{-1}(\pi T t)$), this product takes the value $\delta F_c^{SN} F_c^{SN} = \frac{\mathcal{D}_0}{\mathcal{L}_0} = \frac{1}{3}$.

---

* andrei.pavlov@kit.edu

[1] L. Spietz, K. W. Lehnert, I. Siddiqi, and R. J. Schoelkopf, Primary electronic thermometry using the shot noise of a tunnel junction, Science **300**, 1929 (2003).
[2] P. Février and J. Gabelli, Tunneling time probed by quantum shot noise, Nat. Commun. **9**, 4940 (2018).
[3] S. Larocque, E. Pinsolle, C. Lupien, and B. Reulet, Shot noise of a temperature-biased tunnel junction, Phys. Rev. Lett. **125**, 106801 (2020).
[4] I. Tamir, V. Caspari, D. Rolf, C. Lotze, and K. J. Franke, Shot-noise measurements of single-atom junctions using a scanning tunneling microscope, Rev. Sci. Instrum. **93**, 023702 (2022).
[5] K. Flensberg, Capacitance and conductance of mesoscopic systems connected by quantum point contacts, Phys. Rev. B **48**, 11156 (1993).
[6] K. A. Matveev, Coulomb blockade at almost perfect transmission, Phys. Rev. B **51**, 1743 (1995).
[7] A. Furusaki and K. A. Matveev, Theory of strong inelastic cotunneling, Phys. Rev. B **52**, 16676 (1995).
[8] A. V. Andreev and K. A. Matveev, Coulomb blockade oscillations in the thermopower of open quantum dots, Phys. Rev. Lett. **86**, 280 (2001).

[9] K. A. Matveev and A. V. Andreev, Thermopower of a single-electron transistor in the regime of strong inelastic cotunneling, Phys. Rev. B **66**, 045301 (2002).

[10] Z. Iftikhar, S. Jezouin, A. Anthore, U. Gennser, F. D. Parmentier, A. Cavanna, and F. Pierre, Two-channel Kondo effect and renormalization flow with macroscopic quantum charge states, Nature **526**, 233 (2015).

[11] Z. Iftikhar, A. Anthore, A. K. Mitchell, F. D. Parmentier, U. Gennser, A. Ouerghi, A. Cavanna, C. Mora, P. Simon, and F. Pierre, Tunable quantum criticality and super-ballistic transport in a "charge" Kondo circuit, Science **360**, 1315 (2018).

[12] G. Farahi, C.-L. Chiu, X. Liu, Z. Papic, K. Watanabe, T. Taniguchi, M. P. Zaletel, and A. Yazdani, Broken symmetries and excitation spectra of interacting electrons in partially filled Landau levels, Nature Physics **19**, 1482 (2023).

[13] Y. Hu, Y.-C. Tsui, M. He, U. Kamber, T. Wang, A. S. Mohammadi, K. Watanabe, T. Taniguchi, Z. Papić, M. P. Zaletel, and A. Yazdani, High-resolution tunnelling spectroscopy of fractional quantum Hall states, Nature Physics **21**, 716 (2025).

[14] N. V. Gnezdilov, J. A. Hutasoit, and C. W. J. Beenakker, Low-high voltage duality in tunneling spectroscopy of the Sachdev-Ye-Kitaev model, Phys. Rev. B **98**, 081413 (2018).

[15] A. Manaparambil, A. Weichselbaum, J. von Delft, and I. Weymann, Nonequilibrium steady-state thermoelectrics of Kondo-correlated quantum dots, Phys. Rev. B **111**, 035445 (2025).

[16] D. N. Aristov, Luttinger liquids with curvature: Density correlations and Coulomb drag effect, Phys. Rev. B **76**, 085327 (2007).

[17] M. N. Kiselev, Universal scaling functions for a quantum transport through single-site and double-site charge Kondo circuits, Lecture notes in Physics, in preparation.

[18] T. K. T. Nguyen, M. N. Kiselev, and V. E. Kravtsov, Thermoelectric transport through a quantum dot: Effects of asymmetry in Kondo channels, Phys. Rev. B **82**, 113306 (2010).

[19] T. K. T. Nguyen, J. Rech, T. Martin, and M. N. Kiselev, Noises in a two-channel charge Kondo model (2025), arXiv:2511.02590 [cond-mat.mes-hall].

[20] M. N. Kiselev, Generalized Wiedemann-Franz law in a two-site charge Kondo circuit: Lorenz ratio as a manifestation of the orthogonality catastrophe, Phys. Rev. B **108**, L081108 (2023).

[21] A. I. Pavlov and M. N. Kiselev, Noise signatures of a charged Sachdev-Ye-Kitaev dot in mesoscopic transport (2025), arXiv:2508.13098 [cond-mat.mes-hall].

[22] M. Pustilnik and L. I. Glazman, Kondo effect in real quantum dots, Phys. Rev. Lett. **87**, 216601 (2001).

[23] X. Guo, Q. Zhu, L. Zhou, W. Yu, W. Lu, and W. Liang, Evolution and universality of two-stage Kondo effect in single manganese phthalocyanine molecule transistors, Nat. Commun. **12**, 1566 (2021).

[24] K. P. Wójcik and I. Weymann, Thermopower of strongly correlated T-shaped double quantum dots, Phys. Rev. B **93**, 085428 (2016).

[25] K. Brown, M. Crisan, and I. Ţifrea, Transport and current noise characteristics of a T-shape double-quantum-dot system, J. Phys.: Condens. Matter **21**, 215604 (2009).

[26] D. B. Karki, Wiedemann-Franz law in scattering theory revisited, Phys. Rev. B **102**, 115423 (2020).

[27] C. Mora, C. P. Moca, J. von Delft, and G. Zaránd, Fermi-liquid theory for the single-impurity Anderson model, Phys. Rev. B **92**, 075120 (2015).

[28] A. Oguri and A. C. Hewson, Higher-order Fermi-liquid corrections for an Anderson impurity away from half filling, Phys. Rev. Lett. **120**, 126802 (2018).

[29] C. Mora, P. Vitushinsky, X. Leyronas, A. A. Clerk, and K. Le Hur, Theory of nonequilibrium transport in the SU(N) Kondo regime, Phys. Rev. B **80**, 155322 (2009).